

IMPACT OF CADMIUM SALT CONCENTRATION ON CdS NANOPARTICLES SYNTHESIZED BY CHEMICAL PRECIPITATION METHOD

A. S. NAJM^a, M. S. CHOWDHURY^b, F. T. MUNNA^c, P. CHELVANATHAN^c, V. SELVANATHAN^c, M. AMINUZZAMAN^d, K. TECHATO^e, N. AMIN^{a,f}, MD. AKHTARUZZAMAN^{a,c,*}

^a*Department of Electrical Electronic & Systems Engineering, Faculty of Engineering and Built Environment, Universiti Kebangsaan Malaysia, 43600 UKM Bangi, Selangor, Malaysia*

^b*Environmental Assessment and Technology for Hazardous Waste Management Research Center, Faculty of Environmental Management, Prince of Songkla University, HatYai 90110, Thailand*

^c*Solar Energy Research Institute (SERI), Universiti Kebangsaan Malaysia (UKM), 43600 Bangi, Selangor, Malaysia*

^d*Department of Chemical Science, Faculty of Science, Universiti Tunku Abdul Rahman (UTAR), Perak Campus, Jalan Universiti, Bnadar Barat, 31900 Kampar, Perak D. R., Malaysia*

^e*Center of Excellence on Hazardous Substance Management (HSM), Bangkok, 10330, Thailand*

^f*Institute of Sustainable Energy, Universiti Tenaga Nasional (@The National Energy University), Jalan IKRAM-UNITEN, 43000, Kajang, Selangor, Malaysia*

In this study, cadmium sulfide (CdS) nanoparticles (NPs) were synthesized via chemical precipitation, a facile and cost effective method. The effects of various cadmium salt concentration on the characteristics of CdS NPs has been analyzed to understand the structure properties relationship for optoelectronics applications. XRD, FESEM, Raman Spectra, and UV–Vis has been used to characterize the prepared samples. The optical measurement indicates that there is a direct transition in accordance to energy band gap among 2.36 as well as 2.4 eV. The XRD diffractograms verify that all the films deposited have been polycrystalline of cubic as well as hexagonal structure with superior orientation (111). Analysis of EDX displayed that certain films have been stoichiometric with a small deficiency in sulphur. By optimizing the molar concentration of cadmium ions, the optoelectronic properties of the CdS NPs can be tuned accordingly.

(Received July 19, 2020; Accepted November 2, 2020)

Keywords: Cadmium sulfide, Nanocrystal, Cadmium sulphate, Chemical precipitation method

1. Introduction

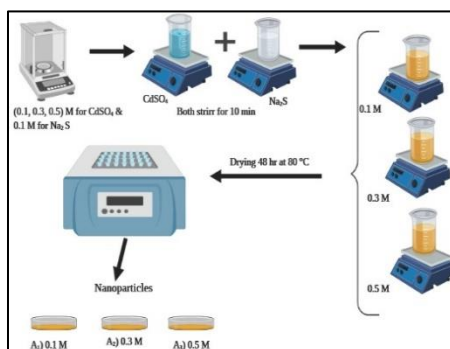
In recent times, transition metal chalcogenides based nanomaterials particularly those belonging to the II–VI semiconductor group had garnered interest in various applications because of their interesting physical properties such as increasing bandgap due to electron confinement [1]–[4]. Among all the binary chalcogenide semiconductor materials, cadmium sulfide (CdS) nanoparticles (NPs) stands out to be the most commonly investigated material mostly due to its wide energy band gap of 2.4 eV [5]. CdS as a semiconductor offers various advantages like accessibility of discrete energy levels, tunable bandgap, optical properties based on size, high chemical stability and simple preparation techniques [6]. Such excellent optoelectronic properties render CdS NP as the material of choice for a wide range of applications such as light emitting diodes [7], photodetectors [8], gas sensors [9] and photovoltaics (PVs) [10].

* Corresponding author: akhtar@ukm.edu.my

Prior to application of the CdS NP in desired system, its optoelectronic properties need to be tuned accordingly and owing to the quantum confinement effect, this is often achieved by manipulating crystallite size. In light of this, innovative synthetic methods for producing CdS NPs have been explored including solvothermal, organosol, thermolysis and reversed micelles. Chemical precipitation method is considered the most suitable among these methods because of its convenience, simplicity, inexpensive and single-step processing [11]. Being a wet chemical method, chemical species that serve as cadmium salt and sulfur source play crucial role in influencing the properties of CdS NPs synthesized via chemical precipitation. By far, cadmium sulphate [12], cadmium chloride [13], cadmium nitrate [14], and cadmium acetate [15] as well as sodium sulphide [16], thiourea [17] and hydrogen sulfide gas are the cadmium and sulfur sources that have been experimented. Apart from the chemical species, molar concentration of these source materials may influence the crystalline structure and consequently, optical and electronic properties of the NPs. Yulisa, et al 2015, investigated the influence of concentrations of ammonium sulfate on the CdS and found at higher concentrations of ammonium sulfate were smoother and the incidence of pinholes was also reduced [18]. Nonetheless, limited studies have been dedicated to comprehend the impact of manipulating concentration of Cd^{2+} ionic species which will be a facile strategy in tuning the properties of CdS. In this study, we used a simple and low-cost synthetic technique for the preparation of CdS NCs based on chemical precipitation with emphasis on the effect of molar concentrations of the cadmium source, CdSO_4 . From various characterizations, we confirmed that essential properties such as bandgap, crystal structure and morphology are dependent of the concentration of CdSO_4 utilized. Hence, by optimizing molar concentrations of the cadmium source, the crystallite size, optical, electrical and structural properties of CdS NPs can be tailored to suit prospective applications.

2. Experimental details

CdS was prepared using a modified method based on Arunraja *et al.*, 2016 [19]. Throughout the current study, aqueous solutions of cadmium sulphate (CdSO_4) (of 99.0% purity) sodium sulphide (Na_2S) (of 99.99% purity) were purchased from the sigma Aldrich (AR), were selected as main precursors for the preparation of CdS nanoparticle. CdS NCs was prepared at room temperature from 0.1 M aqueous solution of Na_2S and varying molar concentration of CdSO_4 namely 0.1, 0.3 and 0.5 M. Each solution dissolved separately in 25 ml of de-ionized and stirred for 10 min. After completely dissolving Na_2S solution was blended with slowly dropping to CdSO_4 solution for 20 min below stirring. No buffer modification has been added. Throughout this process, wet yellow precipitate was collected. Resulting product was dried in an oven for 48 hours at 80 °C. The synthesis process is summarized in Scheme 1.



Scheme 1: Chemical precipitation of CdS NPs

Key chemical reactions that take place in given in the equations 1



The orange colored CdS NP powders were obtained finally and designated as A₁, A₂, and A₃, for 0.1, 0.3 and 0.5 M, respectively. Figure 1 shows the photograph of CdS NPs after the drying process.



Fig. 1 CdS nanoparticles.

3. Result and discussion

3.1. Optical bandgap measurement

To evaluate the efficiency of the solar cells the optical properties play a significant role [20].

Fig. 2 shows the UV–vis absorption spectra of CdS NPs with various concentration of cadmium salt between the wavelength of 300–800 nm.

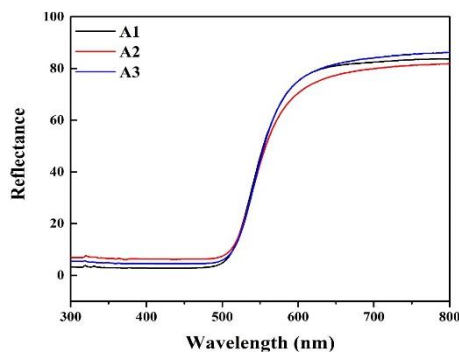


Fig. 2. Impact of different cadmium salt concentration on the optical characteristics of CdS NCs.

As a consequence of increased concentration, it was found that there is a slight change in absorption. As the rapidity of film growth increases with increased concentrations of the impinging particles, it may have deduced that these deviations are due to the specular unformity of the film. Basically, a sharper absorber edge shows fewer defects and impurities in the film. In fact, when CdS begins absorbing light, CdS NCs presented interference patterns through a sudden decrease of transmission nearby the band edge, resulting from the excellent crystallinity of nanoparticles [21]. CdS optical band gap has been evaluated via the Tauc plot depicted in Figure 3. The values of optical band gap is achieved through the dispersion relationship along the essential absorption edge corresponding to the semiconductor direct band gap [22]. Optical band gap (E_{opt}) with optical absorption coefficient (α) are associated in the transition direct semiconductor, as follows:

$$\alpha hv = B(hv - E_g) \quad (2)$$

wherever α is considered to be the absorption factor, hv is the photon energy, E_g constitutes a direct band gap energy, B is a constant, and presuming direct band gap nature of the material, the

significance of $m = 0.5$. The absorption coefficient (α) had determined from the relation $A = I/I_0 = e^{(-\alpha d)}$, or it could analyzing by means of the notable relative reasoned from Beer–Lambert's relation, $\alpha = 2.303A/d$, where d is the path length of the quartz cuvette and A is the absorbance strongminded on or after the UV–visible spectrum [23].

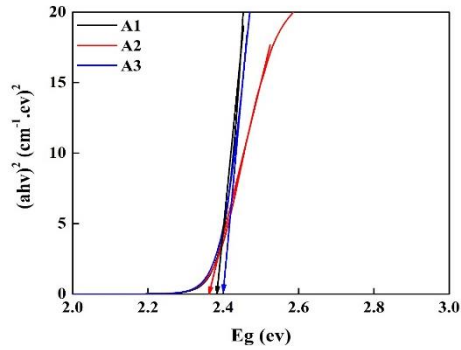


Fig. 3. Variant of $(ahv)^2$ and photon energy for CdS NCs in different cadmium salt concentration.

The comparative bandgap result of CdS NCs are tabulated in Table 1. In regard to the extrapolation of the linear part of the curves to the interception of the horizontal axis, the optical band gaps of all samples were achieved to be between 2,36 and 2,4 eV which is ideal for buffer materials [24]. Remarkably, the observed curves indicate a difference in the direction of the film edge band as a consequence of elevated concentrations of cadmium. A closer analysis of this phenomena reveals that the bandgap energy of 2.4 eV corresponding to the 0.5 M, which is reaches to a saturation energy. The variability in the band gap may possibly be caused by alteration in grain size, stoichiometry, and lattice strain [25]. One possible alternative role of the cadmium species is that the additional Cd vacancies in the lattice may actively dope the band structure through increased concentrations. It is likely that at the time of the deposition phase where the CdS matrix is formed, additional cd vacancies can affect a shift in film stoichiometry. The bandgap energy variations of the crystalline value are expressed in this principle. The optical absorption spectrum of semiconductor materials plays a significant role in supplying fundamental knowledge on its composition and optical bandgap.

Nearby optical bandgap and besides the absorption coefficient curve, there is an exponential part called the Urbach tail. This exponential tail is found in low crystalline, disordered and amorphous materials owing to having localized states that have extended the band gap [26]. Rahal et al. also claimed that the energy of Urbach is associated with film network disorder [27]. In the low photon energy range, the empirical rule for Urbach is defined as the spectral dependency of the absorption coefficient (α) and the photon energy ($h\nu$) as follows:

$$\alpha = \alpha_0 \exp(h\nu/E_U) \quad (3)$$

where α_0 is a constant and the energy of the tail or, occasionally, of Urbach is indicated by E_U , which is dependent upon temperature [28]. By take the two-sided logarithm of the last equation, a straight line equation can be obtained.

$$\ln \alpha = \ln \alpha_0 + (h\nu/E_U) \quad (4)$$

By the slope of the straight plotting line $\ln(\alpha)$ against photon energy incident ($h\nu$), thus, the Urbach energy (E_U) of CdS NCs can be obtained. (see Fig. 4).

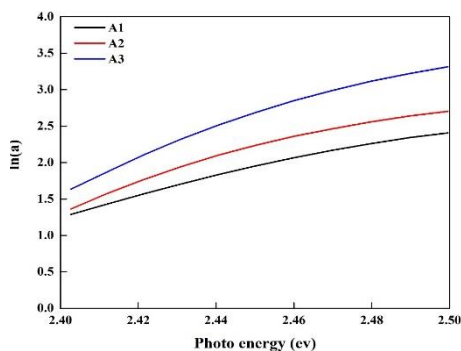


Fig. 4. Urbach energy of CdS NCs.

The slight decrement of the Urbach energy of CdS films is from 0.085 eV to 0.057 eV, which indicated the typical inverse dependence with energy band gap. This attitude could be due to the amount of defect levels generated lower than the conduction band edge of the samples [29]. Figure 5. The lowest value is respective to A3, which this indicates that the crystallinity improves and the defect degree decreases with higher concentration. This finding provides the research community with valuable information that CdS NCs at specific concentration are beneficial for photovoltaic applications.

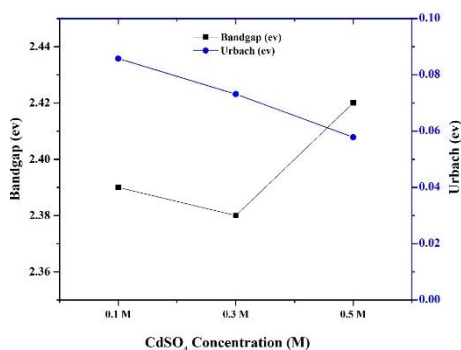


Fig. 5. The variation of bandgap and Urbach energy.

Table 1. Direct band gap energy (E_g) and band tail width (EU) values at a different cadmium salt concentration for CdS NCs.

Molar ratio	E_g (eV)	Eu (eV)
A ₁	2.36	0.085
A ₂	2.38	0.073
A ₃	2.4	0.057

3.2. Raman spectra

Raman spectra of CdS NCs of the differences between 0.1, 0.3, and 0.5 M are highlighted in Fig 2(b).

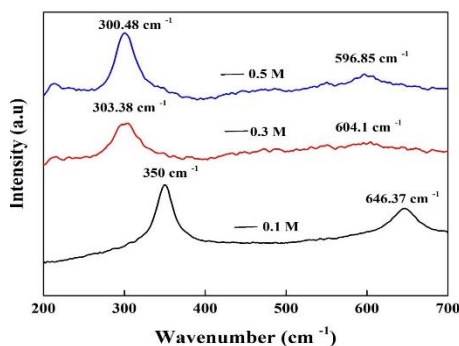


Fig. 6. Raman spectra of CdS NCs at different cadmium salt concentration.

It was observed 0.1 M fundamental single at 350 cm^{-1} longitudinal optical (LO) phonon vibrational modes, and 2LO mode at about 646.37 cm^{-1} . Following the addition of 0.3M and 0.5 M, we observed a small shift at Raman peak with increasing concentration. It is notice that the lower frequency of Raman spectrum has shifted significantly towards higher energy region because of decreasing the particle size of NCs, which may occur due to the electron-phonon interactions [30]. The second-order LO phonon scattering is also noticeable from (596.8 and 646.3 cm^{-1}). Once the particle size grows with the rise in concentration, the intensity of the 2LO line improves, whereas the 1LO line declines, which is in reasonable alignment with the earlier observations reported by Zhang for CdS NCs [31].

3.3. Structural and crystallographic analysis

The XRD patterns were analyzed to explore the crystalline structure of CdS NCs at different cadmium salt concentration. Figure 7 displays that the whole X-Ray diffraction graphs show a broad hump at $2\theta = 26.6^\circ$, showing a strong preferred orientation along the (111) plane and (220) and (311) peaks of the cubic CdS (JCPDS-89-0440) [32].

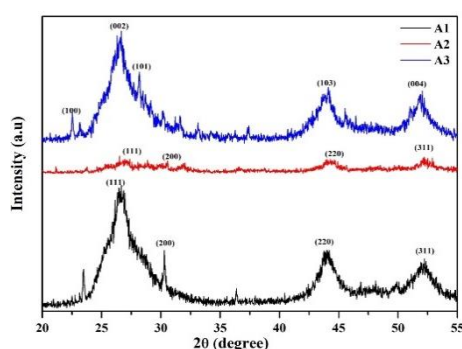


Fig. 7. X-ray diffraction patterns for different cadmium salt concentration.

CdS NCs deposited in a glass can, depending on the preparation conditions, be hexagonal, cubic or mixed structure [33]. CdS display hexagonal and cubic as two crystalline phases. The polycrystalline hexagonal and cubic forms of CdS form random orientations upon deposition and indication several strong diffraction peaks. Table 2 summarizes the values. Thus, it is proven that high purity samples were produced. There is a deterioration of the crystallinity appeared in the film prepared at sample A₂ which will be improved crystallinity by the rise of the cadmium content in the solution, owing to reactants decomposition and the creation of ions essential to the formation and the desorption phenomena [34]. Moreover, in our case the results intensity of sample A₁ show some of Sulfur and Cd that are not react yet which is appearing clearly at an angle $2\theta = 44.9^\circ$ indicating a strong preferred orientation along the (220) plane of Orthorhombic Sulfur (JCPDS-03-065-1436). Sample A₃ blue color spectrum shows 0.5 M concentration X-ray diffraction patterns of CdS NCs. It is not very easy to identify between cubic (1 1 1) and HCP (200), cubic (2 2 0) and HCP (1 1 0). Upon incorporating further concentrations of CdSO₄, new hexagonal structure peaks took place in XRD. This occurrence was supposed to be a phase change in the use of more concentrations of CdSO₄. The combinations of hexagonal and cubic phases were believed to have been altered to the hexagonal phase by the variation of precursor concentration. The different peaks in the diffraction gran were included in the index, and the matching values for the surfaces spacing "d" have been calculated and in comparison with the ordinary values of the JCPDS data [35], [36]. Most striking results to emerge the data is that to changing precursor to the concentration levels higher crystallinity has been observed. The average crystallite sizes of different cadmium salt concentration are estimated by the Debye-Scherrer equation using the strongest peak [4].

$$D = \frac{0.94\lambda}{B \cos \theta} \quad (5)$$

wavelength, and B is the full width at half maximum (FWHM) of the diffraction peak, respectively. The d-spacing for all samples can be estimated from the position of the main peak at 26.6° and by the Bragg condition

$$n\lambda = 2d \sin \theta \quad (6)$$

where, n is the order of diffraction, θ is the diffraction angle, λ is the wavelength of the incident X-ray, and d is the distance between the planes parallel to the axis of incident beam. The calculated crystallite sizes with the d-spacing are given in Table 2.

Table 2. Structural factors of CdS NCs with various cadmium salt concentration.

Sample	CdSO ₄ Concentration (M)	Angle 2θ degree	hkl plane	The interplaner spacing 'd' (nm)	FWHM 'β' peak width (°)	Crystallite size (nm) 'D'
A ₁	0.1	26.61°	(111)	0.334	0.96	8.6
A ₂	0.3	26.75°	(111)	0.332	0.3	28
A ₃	0.5	26.46°	(111)	0.336	1.2	6.8

As can be observed, the values are located in the nanometer range (6.8-28) nm suggesting that the polycrystalline CdS NCs are compose of nanocrystal particles. Compared to the table, Fig. 8 shows the FWHM decreases from 0.1M to 0.3 M and then rises at 0.5 M. Likewise, the size of the crystallite indicates the exact opposite pattern. Also, it could the grain size is regular, and the particle size is uniform you will obtain smooth surface morphology.

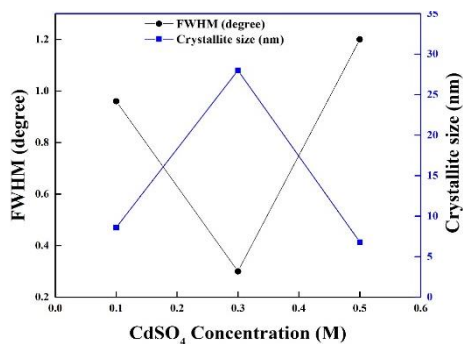


Fig. 8. Variation of the FWHM and dependency on crystalline size with various concentrations on cadmium salt.

3.4. Surface morphology

Field Emission Scanning electron micrographs (FESEM) is a suitable technique to investigate the morphology of the surface, as shown in Fig. 9.

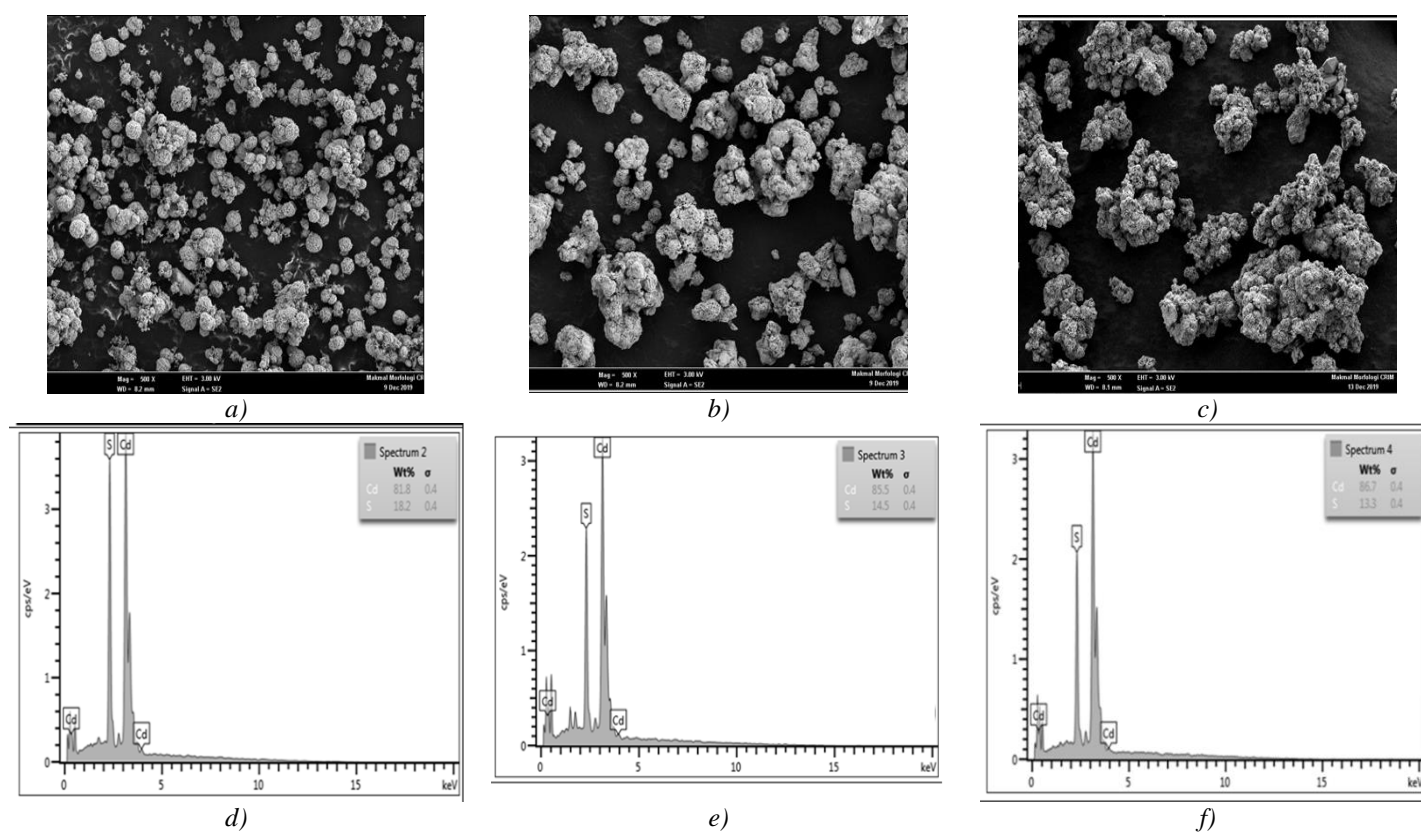


Fig. 9. FESEM micrograph and EDX of CdS NCs different cadmium salt concentration.

When the concentration is altered from 0.1M to 0.5M, sphere size starts increasing and undefined shape grains are also seen on the surface of the sample. In fact, the films are filled by spherical grains, the scale of which reduces and their density rises significantly as concentrations rises. While when the concentration decreases to 0.1M, a small particle is clustered together to procedure larger clusters discreetly dispersed in the films owing to cluster-by-cluster deposition (homogeneous mechanism) as seen clearly in Figures 9(a). Further at 0.3 M, patches of nanostructure grains emerged on the film surface, indicating that this specimen has the largest sphere size in addition to its homogeneous sphere size distribution [37]. Indeed, ion-by-ion deposition (heterogeneous mechanism) is responsible for the structure film formation with increasing concentration to 0.5M, Figure 9 (c) [38]. Yet, some big grains still seem on the surface. A declining behavior of sphere size with dropping concentration was also found by Zhao et al. for CdS thin films grown by CBD method [24], and Lopes et al. for CdS nanospheres synthesized by sonochemical technique [39].

In the material characterization method, it is necessary to fix how the element is distributed laterally and to identify surface inclusions. It is more conveniently accomplished via x-ray or ion probe scanned across the surface and the distinctive elemental signals are used to generate an elementary surface map. Fig. 9 (e, f, and g) displays the EDX spectrum of CdS prepared at different cadmium salt concentration. The spectrum confirms the Cd and S atoms are existing in the film. There are also no impurities in the film that indicate the purity of the films. As concentration of CdSO₄ increase gradually rises the weight ratio, which means that sulfur vacancies (excesses of cadmium) are present on deposited films and serve as donors leading to n-type conductivity. Upon further reducing of concentration, sulfur rich and cadmium deficient specimens are obtained, implying that a divergence from the stoichiometry is found. It can be also declared that it seems an analogous behavior in the alteration between weight and concentrations as anticipated. The weight concentrations from EDX and the considered weight ratio are presented in Table 3.

Table 3. Elemental compositions of CdS NCs in different cadmium salt concentration.

Sample	Cd (wt%)	S (wt%)	[Cd] / [S] (wt%)
A ₁	81.8	18.2	4.49
A ₂	85.5	14.5	5.89
A ₃	86.7	13.3	6.51

4. Conclusions

In current study we synthesized CdS nanoparticles using the chemical precipitation method. Three different concentration of CdSO₄ (0.1, 0.3 and 0.5 M) were employed respectively to investigate the influence of cadmium salt concentration on the optoelectronic characters of CdS NPs. The increase in cadmium salt concentration directly influences the quality and properties of nanoparticles. CdS NPs were achieved with good structural, optical and morphological properties. A dense CdS NCs with proper grain size can be found with 0.1 M CdSO₄.

The optical measurement displays direct transition of energy band gap between 2.36 and 2.4 eV. XRD shown that all the deposited films were polycrystalline of hexagonal and cubic structure with preferential orientation (111). Also, from the X-ray diffraction peaks and surface morphologies micrographs it is estimated that the NP size is between 6.8 to 28 nm as particles assembled to form large clusters at higher CdSO₄ concentration. EDX analysis verified the purity of CdS NPs synthesized by chemical precipitation method. By manipulating concentration of cadmium source, CdS NPs with crystallite size, optical and electronic properties apt for desired application can be attained.

Acknowledgements

The authors also would like to acknowledge the support Universiti Kebangsaan Malaysia (UKM) through DIP-2018-007 research grant and Institute of Sustainable Energy (ISE) of Universiti Tenaga Malaysia (UNITEN) for their support through BOLD2025 Program.

References

- [1] Sumit Pokhriyal, Somnath Biswas, *Applied Surface Science* **501**, 144040 (2019).
- [2] A. Ekinici, S. Horoz, Ö Şahin, *Chalcogenide Letters* **17**(6), 263 (2020).
- [3] Holi, Araa Mebdir, Asla Abdullah Al-Zahrani, Asmaa Soheil Najm, P. Chelvanathan, and N. Amin. *Chemical Physics Letters* (2020): 137486.
- [4] Pei-Ling Li, Yu-Hua Wang, Meng Shang, Lan-Fu Wu, Xiang-Xiang Yu, *Carbon* **159**, 1 (2020).
- [5] M. S. Chowdhury, S. A. Shahahmadi, P. Chelvanathan, S. K. Tiong, N. Amin, K. Techato, N. Nuthammachot, T. Chowdhury, M. Suklueng, *Results in Physics* **16**, 1028391 (2020).
- [6] R. Olvera-Rivas, F. De Moure-Flores, S. A. Mayén-Hernández, J. Quiñones-Galvan, A. Centeno, A. Sosa-Domínguez, J. Santos-Cruz, *Chalcogenide Letters* **17**(7), 329 (2020).
- [7] Rakhi Grover, Ritu Srivastava, Omwati Rana, A. K. Srivastava, K. K. Maurya, K. N. Sood, D. S. Mehta, M. N. Kamalasanan, *Journal of Luminescence* **132**(2), 330 (2012).
- [8] Basudev Pradhan, K. Sharma Ashwani, K. Asim, *Journal of Physics D: Applied Physics* **42**(16), 165308 (2009).
- [9] Alessio Giberti, Davide Casotti, Giuseppe Cruciani, Barbara Fabbri, Andrea Gaiardo, Vincenzo Guidi, Cesare Malagù, Giulia Zonta, Sandro Gherardi, *Sensors and Actuators B: chemical* **207**, 504 (2015).
- [10] Fabiana Lisco, Piotr M. Kaminski, Ali Abbas, Jake W. Bowers, Gianfranco Claudio, Maria Losurdo, J. M. Walls, *Thin Solid Films* **574**, 43 (2015).
- [11] C. H. Ashok, K. Venkateswara Rao, C. H. Shilpa Chakra, V. Rajendar, *International Journal of Pure and Applied Sciences and Technology* **23**(1), 8 (2014).
- [12] H. Metin, R. Esen, *Semiconductor science and technology* **18**(7), 647 (2003).
- [13] Soumitra Patra, Partha Mitra, Swapan Kumar Pradhan, *Materials Research* **14**(1), 17 (2011).
- [14] E. C. De La Cruz Terrazas, R. C. Ambrosio Lázaro, M. L. Mota González, P. A. Luque, S. J. Castillo, A. Carrillo-Castill, *Chalcogenide Letters* **12**(4), (2015).
- [15] Samir Pandya, G., *Int. J. Recent Sci. Res.* **7**(12), 14887 (2016).
- [16] Manjunatha Pattabi, B. Saraswathi Amma, *Solar energy materials and solar cells* **90**(15), 2377 (2006).
- [17] Rifat Hasan Rupom, Rummana Matin, M. S. Bashar, Munira Sultana, M. Rahaman, A. Gafur, M. A. Hakim, M. K. Hossain, M. R. Bhuiyan, F. Ahmed, *American International Journal of Research in Science, Technology, Engineering & Mathematics* **5**, 10 (2016).
- [18] Yulisa Yusoff, Puvaneswaran Chelvanathan, Qamar Huda, Md. Akhtaruzzaman, Mohammad M. Alam, Zeid A. Al-Othman, Nowshad Amin, *Journal of nanoscience and nanotechnology* **15**(11), 9240 (2015).
- [19] L. Arunraja, P. Thirumoorthy, A. Karthik, G. Sriram, V. Rajendran, L. Edwinpaul, *Synthesis and Reactivity in Inorganic, Metal-Organic, and Nano-Metal Chemistry* **46**(11), 1642 (2016).
- [20] Najm, Asmaa Soheil, Norasikin A. Ludin, Mahir Faris Abdullah, Munirah A. Almessiere, Naser M. Ahmed, and Mahmoud AM Al-Alwani. *Journal of Materials Science: Materials in Electronics* **31**, no. 4 (2020): 3564-3575.
- [21] Salah Abdul-Jabbar Jassim, Abubaker A. Rashid Ali Zumaila, Gassan Abdella Ali Al Waly, *Results in Physics* **3**, 173 (2013).
- [22] A. R. Zanatta, *Scientific reports* **9**(1), 1 (2019).
- [23] R. Seoudi, A. Shabaka, W. H. Eisa, B. Anies, N. M. Farage, *Physica B: Condensed Matter* **405**(3), 919 (2010).
- [24] Xiang Hui Zhao, Ai Xiang Wei, Yu Zhao, Jun Liu, *Journal of Materials Science: Materials in Electronics* **24**(2), 457 (2013).

- [25] M. S. Bashar, Rummana Matin, Munira Sultana, Ayesha Siddika, M. Rahaman, M. A. Gafur, F. Ahmed, *Journal of Theoretical and Applied Physics* **14**(1), 53 (2019).
- [26] Shadia J. Ikhmayies, Riyad N. Ahmad-Bitar, *Journal of luminescence* **142**, 40 (2013).
- [27] Achour Rahal, Said Benramache, Boubaker Benhaoua, *Engineering Journal* **18**(2), 81 (2014).
- [28] A. S. Hassanien, Alaa A. Akl, *Superlattices and Microstructures* **89**, 153 (2016).
- [29] S. S. Chiad, W. A. Jabbar, N. F. Habubi, *Journal Of The Arkansas Academy of Science* **65**(1), 39 (2011).
- [30] M. Prasad, Venkata Veera, K. Thyagarajan, B. Rajesh Kumar, In *IOP Conf. Ser. Mater. Sci. Eng.* **149**(1), 2016.
- [31] Hui Zhang, Deren Yang, Xiangyang Ma, Yujie Ji, ShenZhong Li, Duanlin Que, *Materials chemistry and physics* **93**(1), 65 (2005).
- [32] Hui Tao, Zhengguo Jin, Wenjing Wang, Jingxia Yang, Zhanglian Hong, *Materials Letters* **65**(9), 1340 (2011).
- [33] Basudev Pradhan, Ashwani K. Sharma, Asim K. Ray, *Journal of crystal growth* **304**(2), 388 (2007).
- [34] C. D. Lokhande, A. Ennaoui, P. S. Patil, M. Giersig, M. Muller, K. Diesner, H. Tributsch, *Thin Solid Films* **330**(2), 70 (1998).
- [35] O. Vigil-Galan, J. N. Ximello-Quiebras, J. Aguilar-Hernandez, Gerardo Contreras-Puente, A. Cruz-Orea, J. G. Mendoza-Álvarez, J. A. Cardona-Bedoya, C. M. Ruiz, V. Bermudez, *Semiconductor Science and Technology* **21**(1), 76 (2006).
- [36] Faris Abdullah, Mahir, Rozli Zulkifli, Zambri Harun, Shahrir Abdullah, Wan Aizon Wan Ghopa, Asmaa Soheil Najm, and Noor Humam Sulaiman. *Micromachines* 10, no. 3 (2019): 176.
- [37] Salih Yilmaz, Murat Tomakin, Ahmet Unverdi, Abdulaziz Aboghalon, *Gazi University Journal of Science* **32**(4), (2019).
- [38] Samir Pandya, Kamlesh Raval, *Journal of Materials Science: Materials in Electronics* **28**(23), 18031 (2017).
- [39] Paula A. L. Lopes, Maurício Brandão Santos, Artur José Santos Mascarenhas, Luciana Almeida Silva, *Materials Letters* **136**, 111 (2014).